The influence of the colour and the surface area occupied in the camouflage pattern on the reflection index

DOI: 10.35530/IT.076.03.202517

EMILIA VISILEANU
ELENA PERDUM
LAURENTIU DINCA
ADRIAN SALISTEAN
MARIAN CATALIN GROSU

ABSTRACT – REZUMAT

The influence of the colour and the surface area occupied in the camouflage pattern on the reflection index

Textile camouflage structures designed for weather protection, combat suits, and military uniforms for land forces are defined by their physical, mechanical, and optical properties. An analysis of the statistical populations of reflection within the wavelength range of 860–1200 nm revealed the degree of dispersion in the measured values. A novel method was developed to determine the weight of monochromatic areas on a multi-coloured surface. Various camouflage textile structures were examined to investigate the correlation between reflection indices and the weight of the single-coloured regions. Several parameters were identified, including the colour index, the range of colour reflectance, the area covered by each colour, and the weight of the colour-covered region. To assess the degree of reflection for each colour within the spectral range of 860–1200 nm, the median of the reflection values was calculated, as it provides a more representative measure of the overall reflective properties. The frequency distribution of these values was analysed, leading to the establishment of a ranking of camouflage types based on their reflection coefficients, starting with the lowest reflection value. Regression curves were derived for the reflection index values at wavelengths between 860–1200 nm, with increments of 10 nm. These initial regression curves, along with those weighted by colour area, include regression equations for the analysed textile structure variants. These equations enable the calculation of the regression index as a function of wavelength.

Keywords: *camouflage textile structures, reflection, wavelength range, optical properties, regression curves*

Influența culorii și a suprafeței ocupate în modelul de camuflaj asupra indicelui de reflexie

Structurile textile de camuflaj destinate protecției împotriva intemperiilor, echipamentelor de luptă și uniformelor militare pentru forțele terestre sunt caracterizate prin proprietăți fizice, mecanice și optice specifice. În cadrul acestui studiu, analiza populațiilor statistice de reflexie în intervalul de lungimi de undă 860–1200 nm a evidențiat gradul de dispersie al valorilor măsurate. A fost propusă o metodă inovatoare pentru determinarea ponderii zonelor monocromatice pe o suprafață policromă. Au fost investigate diverse structuri textile de camuflaj pentru a stabili corelații între indicii de reflexie și ponderea zonelor colorate uniform. Parametrii analizați au inclus indicele de culoare, intervalul de reflectanță al fiecărei culori, suprafața acoperită de fiecare culoare și ponderea corespunzătoare a fiecărei regiuni colorate.
Pentru a evalua nivelul de reflexie al fiecărei culori în intervalul spectral menționat, a fost utilizată mediana valorilor de reflexie, considerată un indicator mai reprezentativ al comportamentului optic general. Distribuția frecvenței valorilor de reflexie a permis realizarea unei clasificări a tipurilor de camuflaj în funcție de coeficientul de reflexie, începând cu valorile cele mai scăzute. Curbele de regresie au fost construite pentru indicii de reflexie corespunzători lungimilor de undă cuprinse între 860 și 1200 nm, la un pas de 10 nm. Atât curbele de regresie inițiale, cât și cele ponderate în funcție de suprafața acoperită de fiecare culoare, includ ecuații de regresie pentru variantele analizate ale structurilor textile. Aceste ecuații permit calculul indicelui de regresie în funcție de lungimea de undă, oferind o bază solidă pentru proiectarea avansată a materialelor de camuflaj.

Cuvinte-cheie: *structuri textile de camuflaj, reflexie, interval de lungimi de undă, proprietăți optice, curbe de regresie*

INTRODUCTION

Protective textiles used in military applications must fulfil a variety of functional requirements, including durability, resistance to environmental conditions and ballistic threats, while also being comfortable and lightweight. The Research and Markets report on the Smart Textiles for Military Equipment Market, by Type, Application, End-User, and Region (2024–2032), highlights that the global smart textiles market for military applications reached USD 890.4 million in 2023 and is projected to reach USD 2,535.5 million by 2032, registering a growth rate of 12.33% during this period. By 2027, the global military smart textiles market is expected to be dominated by the camouflage sector [1].

Camouflage has always played a major role in military operations. Its purpose is to blend combat suits and equipment with the natural environment, reducing the visibility of soldiers and their tools. Today, camouflage involves more than just design and colour; it requires several key elements. For example, camouflage effective in daylight may be rendered useless when viewed through night-vision technology. In such cases, an infrared (IR) signature becomes essential. Defining an exact IR reflectance corridor for each colour in a pattern is crucial for good daytime camouflage that remains effective in twilight or complete darkness at night [2]. In addition, these textiles must perform well under various environmental conditions and across a range of wavelengths on the electromagnetic spectrum. As infrared sensing technology advances, the focus of protective textile research has shifted from visible camouflage to camouflage in the IR region. Smart textiles, capable of monitoring and reacting to the wearers or environmental stimuli, have been incorporated into protective fabrics to enhance camouflage in the IR spectral range [2–4].

Conducting military operations requires a degree of stealth to operate covertly and therefore avoid detection. Traditionally, being able to blend into the surrounding environment under daylight was the key, when visual camouflage was king; however, as times have progressed, so has technology; enter the Infrared camera and night vision goggles. With the rapid development of surveillance and acquisition devices, it became imperative to develop camouflage textiles that could protect objects from detection by various sensors in a wide spectral range. As sensor systems continue to be refined, the performance of camouflage materials must be continually updated [5], reducing thermal emissions for various applications. Objects emit infrared radiation detectable by devices, making military targets easily identifiable. Infrared camouflage mitigates detection by lowering an object’s infrared radiation, achieved by methods such as reducing surface temperature, which is crucial in designing military tents with IR camouflage, considering water repellence and antibacterial features [6]. IR protection involves using materials or coatings that either absorb or reflect infrared radiation, thereby reducing the heat signature of soldiers.

The latest breakthroughs in military equipment will be implemented soon, and by 2025 the military will have a smart uniform, able to instantly adapt its colour in perfect correlation with the geographical area and fauna, but also to change the insulation properties to ensure an optimal temperature depending on the environmental conditions specific to the areas in theatres of operations where the military is operating. To camouflage military equipment and personnel, synthetic green pigments are incorporated into the coating materials. However, conventional green pigments do not resemble chlorophyll in the infrared region. They absorb infrared light while chlorophyll reflects it. Thus, chlorophyll appears to be the only known organic IR-reflecting pigment; this explains why the shade of trees is cooler than the surrounding area during very hot summer days. As a result, an improperly rendered camouflage colour appears black in contrast to a light-coloured background when viewed with infrared equipment. How do infrared reflective materials (IRR-reflective materials) work? The IRR technology works through visual disruption, caused by the multi-layered infrared signatures for each colour within the print pattern, which have a specific reflective wavelength to blend in with colours in the infrared spectrum for the specific location garments are intended to be worn [7]. The result is greatly reduced visibility of the wearer at night with reflectance to mimic the same wavelengths as snow, rocks, differing urban environments, trees and other green vegetation; while in regular light conditions, you will still have the traditional camouflage patterns to blend into your surroundings [8].

MATERIALS AND METHODS

Layout

Camouflage textile materials were produced using a printing machine with rotating cylinders and inks containing pigments that provide various IR (infrared radiation) shielding levels. The physical-mechanical characteristics of the textile structures Group M are presented in table 1 and table 2, for Group G

Table 1

No.	Characteristics/Variant		UM	M1-A	M2-N	M3-A	M4-N	M5-T
1	Weight		g/m^2	172.66	183.48	229.8	221.28	231.74
2	Density	U	Yarn no./ 10 cm	760	770	500	496	480
		B		270	290	236	240	240
3	Maximum breaking strength	U	N	1443.38	1536.39	1674.34	1708.10	1576.57
		B		1024.20	1100.98	690.02	621.41	652.59
4	Elongation at break	U	%	40.48	45.30	48.08	48.49	47.15
		B		42.63	37.24	14.97	14.61	12.50
5	Resistance to deformation		kPa	726.9	584.7	433	382	387.2
			mm	46.3	36,2	25.0	22.9	23.1
6	Bundle			D2/2	D2/2	D3/1	D3/1	D3/1
7	Water vapour permeability		%	6.3	5.8	30.0	30.8	30.2
8	Air permeability		l/m^2/s	0.0 Impermeable	0.0 Impermeable	258.4	210.1	309.7
9	Abrasion resistance		cycle/no.	>100.000				
10	Fibrous composition		%	69%PA/22%Pes/PU+PTFE		60%Cotton/40%PA		

Table 2

No.	Characteristics/Variant		UM	G1-N	G2-A	G3-T	G4-T	G7-T	G9-A
1	Weight		g/m^2	177.3	178.8	215.1	209.3	151.0	154.1
2	Density	U	Yarn no./ 10 cm	640	640	394	440	614	610
		B		300	300	214	236	292	290
3	Breaking strength	U	N	1191.9	1284.9	1070.1	1289.0	996.2	985.2
		B		779.4	809.7	630.2	990.4	834.4	742.7
4	Elongation at break	U	%	50.3	51.8	13.6	43.1	46.0	44.4
		B		42.3	19.5	14.93	28.2	28.4	-
5	Resistance to deformation	kPa		654.1	746.2	507.5	556.3	679.9	660.2
		mm		44.0	51.4	25.9	27.3	46.9	49.0
6	Bundle			D2/2	D2/2	D3/1	D3/1	D3/1	D3/1
7	Water vapour permeability		%	5.1	5.1	30.4	21.4	2.9	4.0
8	Air permeability		$l/m^2/s$	8.59	7.93	199.2	153.9	0.0 Imper.	0.0 Imper.
9	Abrasion resistance		cycle/no.	>100000	>100000	70.000 Broken yarns	90.000 Broken yarns	>100000	>100000
10	Fibrous composition		%	80%PA/20%PU		60%Cotton/40%PES		65 %PA+35%PU	

produced by the ST *(Technical specifications)* for Weather Protection Suits (M1, M2, G1, G2, G7, G9) according to ST *(Technical Specification)* 1542/2016 and Combat Suits: (M3, M4, M5, G3) according to ST 1729-2018 for ground forces.

The structures in the M range generate two groups of fibrous compositions: 69%Poliamide/22%Polyester/Polyurethane + Polytetrafluorethylene) (M1 and M2) with mass ranging from 172.66 g/m^2 (M1) to 183.48 g/m^2 (M2), and 60%Cotton/40%Polyamide (M3-M5) with mass ranging from 221.28 g/m^2 (M4) to 231.74 g/m^2 (M5). The structures in the G range generate three groups of fibrous compositions: 80%PA/20%Polyester/Polyurethane (G1 and G2) with mass ranging from 177.3 g/m^2 (G1) to 178.8 g/m^2 (G2), and 60%Cotton/40%Polyester (G3-G4) with mass ranging from 209.3 g/m^2 (G4) to 215.1 g/m^2 (G3), and 65%Polyamide/35%Polyuretane (G7 and G9) with mass ranging from 151.0 g/m^2 (G7) to 154.1 g/m^2 (G9).

ID reflectance

The determination of IR reflectance is a spectrophotometric method used to measure the reflectance on the surface of a flat material (e.g., textile material) as a function of the wavelength of incident IR radiation. IR spectroscopy is a versatile analytical technique that can be applied across a wide range of research and industrial applications. Reflectance is an optical property of the material and represents the ratio (as a percentage) between the intensity of the incident radiation on the surface of the tested material and the total intensity of the radiation reflected in all directions.

Reflection occurs when electromagnetic radiation (e.g., IR) is redirected back into the originating medium after striking the surface of the tested material. This surface separates two different optical media: the first being the source of the incident radiation (air), and the second being the tested material.

One method to measure is 3D Imaging and Light Scattering Techniques that use 3D imaging technology, often combined with lasers or other light sources, to understand how light interacts with a fabric's surface at different angles [9–12].

For textile materials, reflection typically occurs on rough surfaces, which tend to diffuse the radiation, unlike materials with lower roughness.

For such measurements, an integrating sphere is required inside the spectrometer to obtain the reflectance spectrum of the tested surfaces. The equipment used was a UV-VIS-NIR Spectrophotometer, Lambda 950 model, Perkin Elmer, with a spectral range of 185–3300 nm, which includes an integrating sphere unit.

Determination of the proportion of single-colour areas on a multicolour surface

Measuring the optical properties (e.g., reflectance, absorbance) on a multicolour material surface for each colour individually leads to a global characterisation of the material when the measurement results are averaged over a sufficiently large area to be representative of the material under investigation. This is achieved by weighting the values of the measured optical quantities for each colour, thus obtaining a weighted average value that characterises the entire surface of the material in terms of its optical properties. The weights used in this calculation are precisely the contribution weights of the areas of each colour to the total averaging area.

The determination of the average reflectance was carried out using an innovative and original method, consisting of: a) measuring the dimensions and scanning the flat material; b) identifying and indexing the monochromatic areas; c) calibrating the length in the software that calculates the geometric parameters of the objects traced from the images; d) outlining the edges of the region of interest using a closed polyline in the same software, which calculates its area (the value considered as the total area for the subsequent determination of the area weight); e) outlining the edges of each subzone that makes up each monochromatic area using a closed polyline in the same software, except for one monochromatic area to increase processing efficiency; f) calculating the area for the untraced monochromatic zone by subtracting the sum of the other monochromatic areas from the total area; g) determining the weight of each monochromatic zone.

RESULTS AND DISCUSSIONS

Statistical analysis of the variability of the reflection index

To characterise the populations of IR reflection index values in the wavelength range of 860–1200 nm, for each colour and textile structure variant, a specialised program (IBM-SPSS) was used that allowed a rigorous description of the distributions resulting from the tests performed. The mean, variance, standard deviation, median, and quartiles were calculated for the obtained reflection index values, along with skewness and kurtosis to assess asymmetry and highlight cases where interventions might be necessary. The mean, variance, standard deviation, median, and quartiles, along with skewness and kurtosis, are examples of the reflection variable of the colours in the M1 textile structure in table 3. Histograms and box plot graphs of the reflection variable for a colour in the M1 textile structure are shown in figure 1, *a* and *b* (one colour).

From table 3, it can be observed that:

- the skewness indicators for reflexive colours have positive values for light blue (5.514), dark blue (5.486), blue (0.530), indigo (5.451), and green (0.496), which highlights the extent to which the mean deviates from the median. As a result, the normal distribution curves deviate from the centre, shifting to the right;
- the kurtosis indicators show positive values for the colours: light blue (31.465), dark blue (31.219), and indigo (30.904), with the curves being leptokurtic. Negative values are shown for the colours blue (0.836) and green (–1.063), with the curves being platykurtic.

From figure 1, it can be observed that for the colour blue (M1), the reflection variable shows a distribution where 50% of the values are skewed to the left, with the median being positioned towards the lower part of the box. This indicates that lower values of reflection are predominant.

The study of the statistical populations of reflection in the wavelength range of 860–1200 nm highlighted the following aspects for the analysed variants:

- the highest uniformity of reflection values was recorded for variant G3 (ground forces), which contains masking colours of black and shades of grey arranged in regular geometric shapes (rectangle, square, rhombus, etc.);
- the highest non-uniformity of reflection values is presented by variant M5 (ground forces), a combination of khaki, beige, brown, and dark brown colours arranged in irregular shapes; significant non-uniformities of reflection are also presented by variants G7 (ground forces) and M1 (air forces).

To obtain the weighted average value of reflection under the method described above, an example is provided with the steps followed and the corresponding illustrations.

Table 3

REFLECTION VARIABLE OF THE COLOURS IN THE M1 TEXTILE STRUCTURE

Variable		M1 light blue	M1 dark blue	M1 blue	M1 indigo	M1 green
M1	Valid	35	35	35	35	35
	Missing	0	0	0	0	0
Mean		1362.2305	1099.5792	95.5138	1047.8490	93.3396
Std. Error of Mean		926.62797	735.08639	43624	699.75685	56626
Median		62.8588	47.1150	94.5708	44.4902	91.9061
Mode		–34.84*	–12.44*	91.55*	18.06*	89.94*
Std. Deviation		5482.00502	4348.82975	2.58060	4139.81734	3.35005
Variance		30052378.997	18912320.194	6.661	17138087.608	11.223
Skewness		5.514	5.486	530	5.451	496
Std. Error of Skewness		396	396	396	396	396
Kurtosis		31.465	31.219	–838	30.904	–1.063
Std. Error of Kurtosis		778	778	778	778	778
Range		32143.88	25459.51	9.07	24153.63	11.30
Minimum		–34.84	–12.44	91.55	18.06	87.94
Maximum		32109.04	25447.07	100.63	24171.69	99.23
Sum		47678.07	38485.27	3342.98	36674.72	3266.89

Note: *A Multiple mode exists. The smallest value is shown.

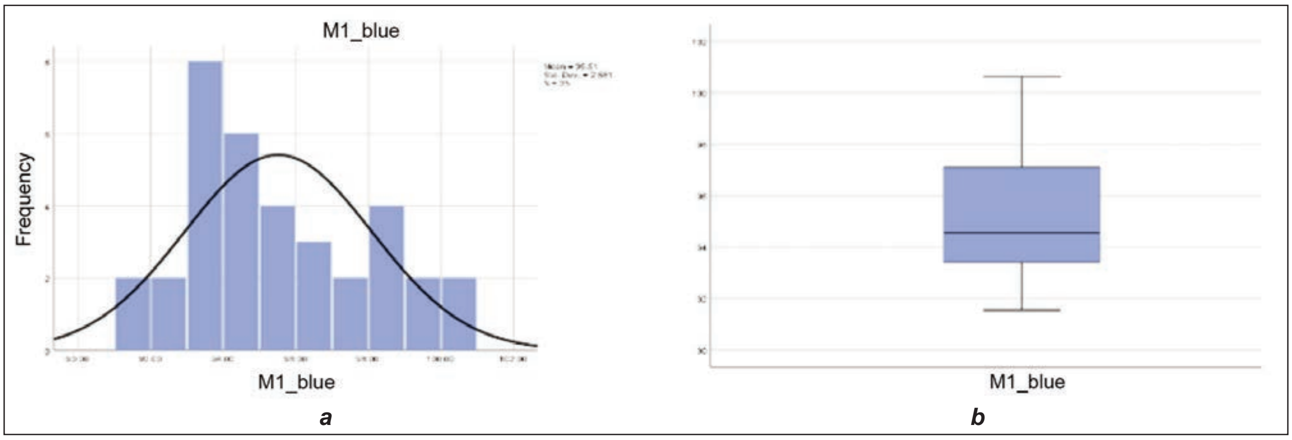

Fig. 1. Graphical representation: *a* – histogram; *b* – box plot graph of the reflection variable (colour variant M1)

Size measurement and scanning
This step allowed the lateral dimensions of 198×175 mm^2 to be identified using a ruler and a flatbed scanner for the material in figure 2, *a* (Scan image of planar material).

Identification and indexing
This step provided the scanned image from figure 2, *b* which illustrates seven colours identified with indices from 1 to 7.

Length calibration
The length calibration was performed; this step consisted of the setting of the correspondence factor between pixel counts and length (11.97 pixels/mm), using the measured size values of the planar material and the same sizes in pixels according to the software. After that, the edge plotting of the entire analysed area was done, providing an image framed into a rectangular boundary (figure 2, *c*). The area of this region was determined (33998.63 mm^2), taking the role of the total area in subsequent weight calculation.

An image with the plot of each subzone of each single-colour zone (exception for colour 5) was obtained (figure 2, *d*), leading to the software measurement of the single-colour areas. The area corresponding to the colour 5 was calculated by subtracting the total area of colours 1, 2, 3, 4, 6 and 7 from the entire analysed area. After that, the contribution ratio of each single-colour zone from the analysed area was

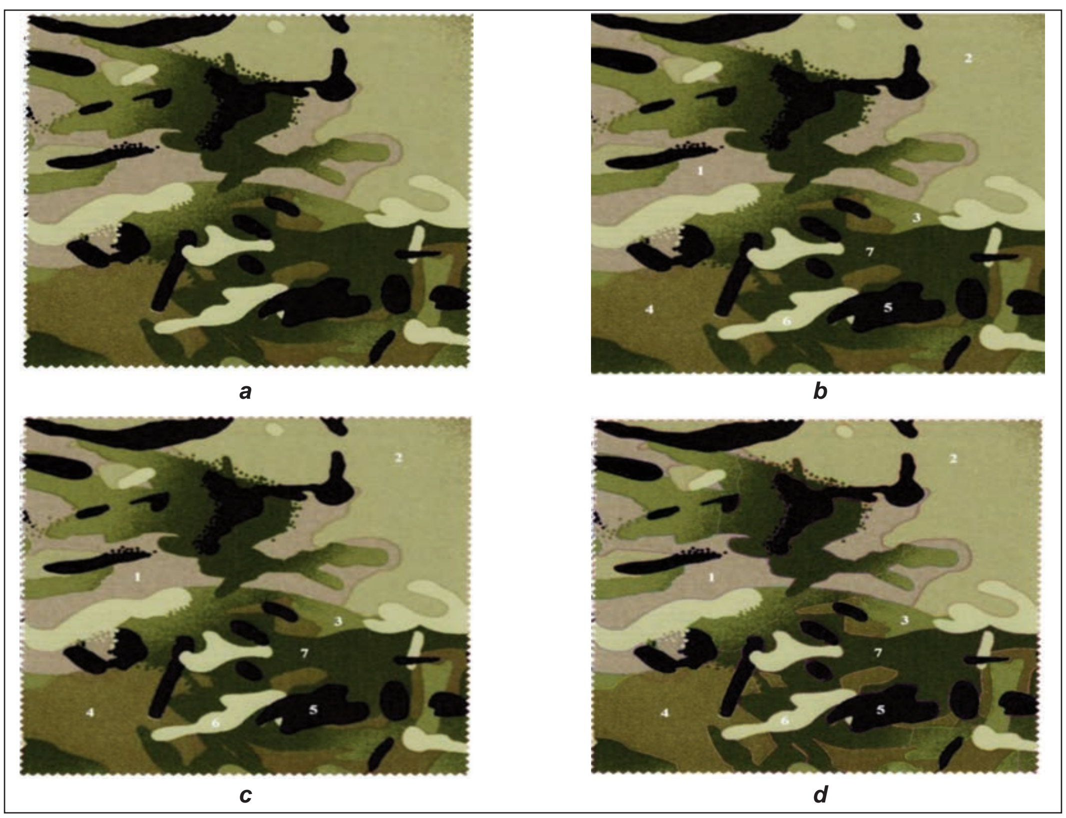

Fig. 2. Photos of: *a* – scan image of planar material; *b* – size measurement and scan; *c* – length calibration and edge plotting of entire analysed area; *d* – edge plotting of each subzone; area calculation for each colour

determined (the ratio of the single-colour area to the total area).

Tracing the region of interest boundary

This step resulted in obtaining the image figure 2, *c* – region of interest bounded by a closed polyline (in red), by tracing the boundary of the region of interest. The area of this region (33,998.63 mm^2) was also generated, considering the total area for the subsequent determination of the weighting. Drawing the boundaries of each subzone and calculating the area for each colour. This step led to obtaining the image (figure 2, *d* – image with each subarea marked with colour) with the graphical representation of each subzone within each monochrome area (except for colour 5).

Additionally, the area values for the monochrome zones were generated by the software after the drawing. The area corresponding to colour 5 was calculated through the subtraction mentioned above.

Determining the weight

This step provided the contribution ratio of each monochrome zone to the area of interest (the ratio between the monochrome area and the total area). The weights are presented in table 4.

Table 4

Monochrome area index	Area (mm^2)	Weight
1	3855.36	0.11
2	6937.39	0.20
3	3932.18	0.12
4	4134.69	0.12
5	5097.54	0.15
6	2751.82	0.08
7	7289.64	0.21

Correlation of reflection indices with the weighting of single-colour areas

To identify the correlation between the reflection indices and the weights of the areas of a single colour, experiments were carried out on the textile structures: M5, G3, G7, G4, G8, M3, G2, G1. Table 5 shows the range of the reflectance of the colours in the spectral band 860 ÷ 1200 nm and the weight of the area covered in the investigated area (%) by each colour for the variants of masking textile structures M1, M3, M5 and G1, G2, G3, G4, G7, G9.

Determination of median values for the reflection index of textile structures

The data series for “Measured Reflection” for each camouflage type was weighted by the percentage of colour coverage in the camouflage pattern of the sample. This resulted in a spectral distribution, also represented graphically, of the reflection coefficients for each camouflage model. Additionally, the regression equations for the data series obtained are displayed on each graph.

For each wavelength, the colour with the lowest reflection coefficient was analysed. From the data series, the frequency of appearance for each colour was calculated, and then the top colours (for all 39 colours) with the lowest reflection coefficient across the entire spectral band were extracted. A similar process was followed for the colours in the second data set, producing the top colours/samples (for the 16 analysed colours) with the lowest reflection coefficient across the entire spectral band.

To assess the reflection degree of each colour across the entire spectral band, the median values were calculated due to the high dispersion of the data. At certain wavelengths, the pigment used has a very strong reflectivity, so the average does not correctly represent the entire spectral band. Therefore, the median value is a much more representative variable of the total reflective qualities. A ranking of the colours based on their reflection index was obtained: black (G3) = –12.0%; brown and dark brown (G7) = 23.52% and 23.46%, respectively; khaki and brown = 32.1% and 32.32% (M5), etc. (figure 3).

Similar to the previous case, the frequency of values was analysed, and a ranking of the types of camouflage analyzed (8 types of camouflage) was obtained, starting with the lowest reflection coefficient recorded for the M5 variant (46.94%), followed by G7 (47.03%) and M3 (53.01%) (figure 4).

Fig. 3. Ranking of the colours

Table 5

DISCRIMINANT VALIDITY (THE FORNELL-LECKER CRITERION)					
Variant	**Colour**	**The colour indicator used in the image of the investigated area**	**Colour reflectance range in the spectral band 860 ÷ 1200 nm (%)**	**Area weight of colour in the investigated area (%)**	**Area covered by colour in the investigated area (pixel²)**
M1	Light blue	M1-a	–34 ÷ 32109	8.98	655697.00
	Dark blue	M1-b	–12 ÷ 25447	28.52	2082281.00
	Blue	M1-c	91 ÷ 100	15.20	1109507
	Indigo	M1-d	18 ÷ 24171	28.27	2064421
	Green	M1-e	87 ÷ 99	19.03	1389346
M3	Dark blue	M3-a	–237 ÷ 180	25.80	1893927.00
	Light blue	M3-b	–4 ÷ 181	4.60	337348
	Indigo	M3-c	–106 ÷ 184	31.18	2288847
	Blue	M3-d	18 ÷ 91	16.69	1225205
	Green	M3-e	–561 ÷ 1303	21.74	1595721
M5	Khaki	M5-a	–17 ÷ 189	31.29	2285608
	Green	M5-b	34 ÷ 291	21.38	1561865
	Beige	M5-c	43 ÷ 103	6.95	507429
	Brown	M5-d	–192 ÷ 1133	19.99	1460095
	Light brown	M5-e	–45 ÷ 36110	20.39	1489485
G1	Black	G1-a	81 ÷ 100	18.44	1452798.00
	Indigo	G1-b	85 ÷ 100	36.33	2862318.00
	Blue	G1-c	89 ÷ 100	5.94	468216.00
	Dark blue	G1-d	85 ÷ 100	20.07	1581624.00
	Light blue	G1-e	89 ÷ 101	19.21	1513701.00
G2	Light blue	G2-a	89 ÷ 101	17.19	1220144.00
	Green	G2-b	84 ÷ 99	34.45	2446195.00
	Indigo	G2-c	85 ÷ 99	16.85	1196675
	Bleu	G2-d	90 ÷ 102	6.63	470458
	Dark bleu	G2-e	86 ÷ 100	24.88	1766544.00
G3	Black	G3-a	–142 ÷ 5251	19.75	1549670.00
	Gray	G3-b	84 ÷ 99	4.59	359999.00
	Light grey	G3-c	90 ÷ 99	15.40	1207997.00
	Dark gray	G3-d	77 ÷ 98	60.26	4727518.00
G4	Beige	G4-a	87 ÷ 99	7.49	514589
	Khaki	G4-b	84 ÷ 99	36.16	2485727
	Light brown	G4-c	–7 ÷ 29000	16.18	1112006
	Dark brown	G4-d	84 ÷ 99	18.25	1254883
	Green	G4-e	–7 ÷ 29000	21.93	1507355
G7	Beige	G7-a	89 ÷ 100	7.27	517592.00
	Brown	G7-b	–43 ÷ 14827	29.92	2129993.00
	Light brown	G7-c	87 ÷ 99	22.46	1598952.00
	Dark brown	G7-d	–58 ÷ 15350	16.21	1153737.00
	Green	G7-e	–1.1 ÷ 22732	24.15	1719336.00
G9	Light blue	G9-a	–12.5 ÷ 85.7	18.93	1361918.00
	Green	G9-b	–35.2 ÷ 86	27.55	1982078.00
	Indigo	G9-c	–50.4 ÷ 112.4	21.03	1512614
	Light blue	G9-d	–2.4 ÷ 1623356.6	7.65	550511
	Dark blue	G9-e	–11.3 ÷ 84	24.84	1786849.00

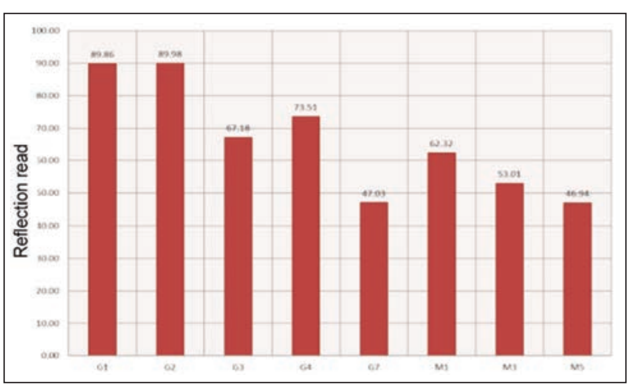

Fig. 4. Measurement model: Reliability

Regression analyses

In figure 5, the initial regression curves are presented, along with the regression curves weighted by the colour areas for the reflection index values at wavelengths from 860 to 1200 nm in 10 nm steps. The linear regression equations with the regression coefficients for the analysed textile structure variants are also shown, which allows the calculation of the regression index as a function of a certain wavelength.

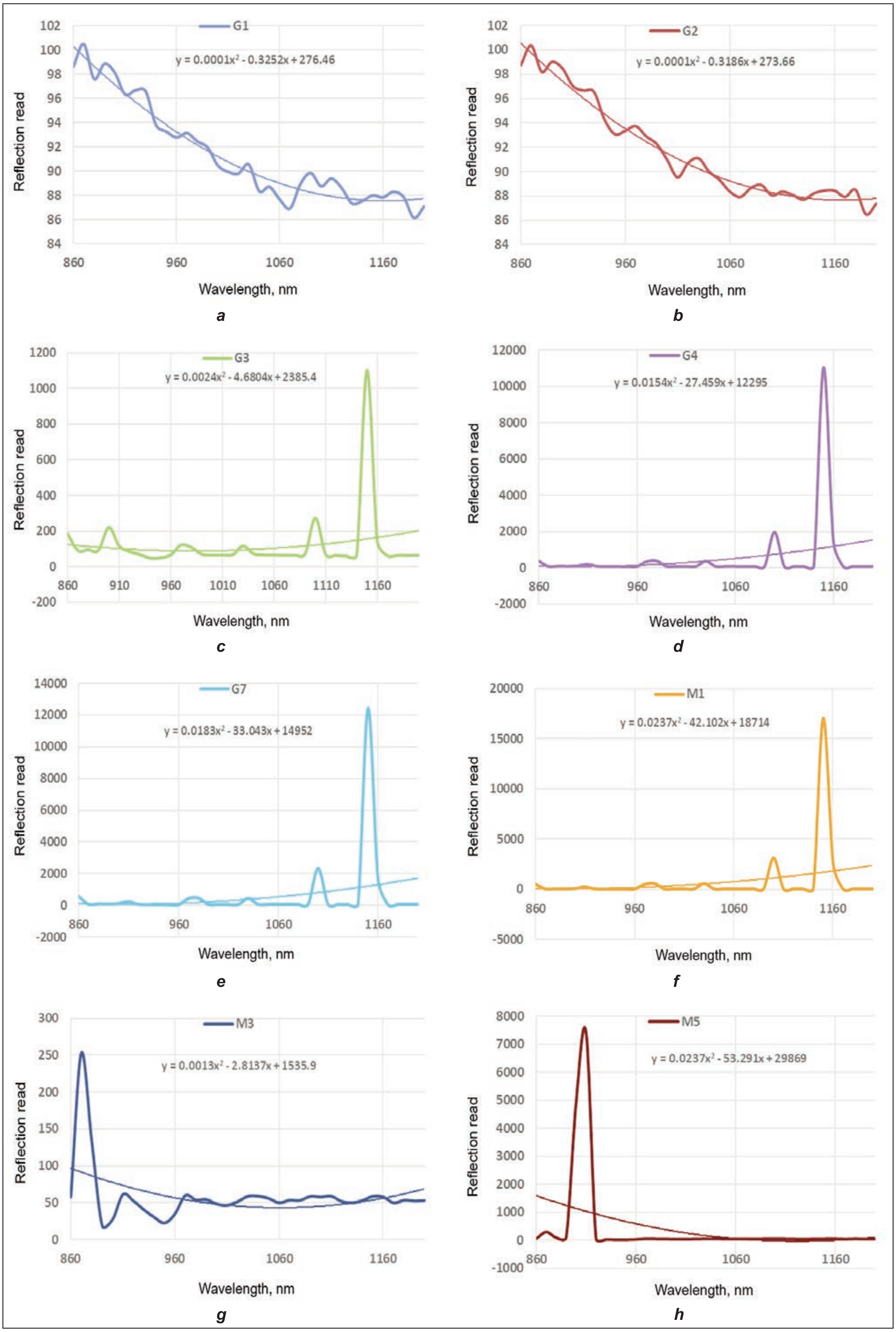

Fig. 5. Regression curves of: *a* – G1; *b* – G2; *c* – G3; *d* – G4; *e* – G7; *f* – M1; *g* – M3; *h* – M5

CONCLUSIONS

Different camouflage variants (M1, M2, M3, M4, M5, G1, G2, G3, G4, G7, G9) with different fibrous compositions, such as a blend of polyamide, polyester, and polyurethane, and with specific properties, such as resistance to abrasion, water vapour permeability, and air permeability are analysed. The determination of IR reflectance is done using a spectrophotometric method, measuring the amount of infrared radiation reflected by the textile material. This helps assess how well the material performs in the IR spectrum, contributing to its effectiveness in camouflage.

The correlation between reflection indices and area weighting for different colours revealed that certain colours, like dark blue and indigo, cover a significant portion of the total area (up to 36% for indigo in the G1 variant). This is important for creating textiles that provide maximum camouflage in both visible and IR spectrums.

The G1 (Ground Forces) variant, with shades like indigo and dark blue, showed a promising combination of high reflectance in the IR range, which can be important for avoiding detection in the infrared spectrum.

The research underlined the importance of designing camouflage patterns that are effective across multiple spectral ranges, especially given the rise of infrared sensors. The textile structures tested showed varying degrees of success in blending into environments when viewed through IR devices, underscoring the necessity for smart textiles to adapt to both visible and infrared camouflage.

Infrared Reflective (IRR) technology, as evidenced in the tests, contributes to reducing visibility in the infrared spectrum by mimicking the natural IR signature of the environment. Materials like khaki and green were found to be more effective in specific environments like forests and urban terrains.

Moving forward, smart textiles that can dynamically adjust to environmental conditions (such as changing colour or insulating properties) will significantly enhance military operations, particularly in covert missions. These adaptive textiles could be designed with further enhancements in their IR reflective properties and resistance to environmental factors.

In conclusion, the study highlights the importance of infrared reflective properties in military camouflage and the critical role of uniformity in reflectance for consistent performance. The findings suggest that a balance between durability, comfort, and effective camouflage across both visible and infrared spectrums is essential for the next generation of military protective textiles.

ACKNOWLEDGEMENTS

This work was carried out through the "Nucleu" Programme within the National Research Development and Innovation Plan 2022–2027, carried out with the support of MCID, project no. 6N/2023, PN 23 26, project title "Intelligent equipment to ensure the survival of combatants in operational conditions", Acronym: IRHEM.

REFERENCES

[1] *Global Military Smart Textiles Market 2024 by Manufacturers, Regions, Type and Application, Forecast to 2030*, SKU ID: GIR-26322062, Jan 2024, 95, Available at: https://www.researchreportsworld.com/global-military-smart-textiles-market-26322062 [Accessed on January 2025]

[2] Brayley, M.J., *Camouflage Uniforms: International Combat Dress, 1940–2010*, Ramsbury: Crowood, 2009, ISBN 978-1-84797-137-1

[3] Steffens, F., Gralha, S.E., Ferreira, I.L.S., Oliveira, F.R., *Military textiles – an overview of new developments*, In: Key Engineering Materials, 2019, 812, 120–126, https://doi.org/10.4028/www.scientific.net/kem.812.120

[4] Degenstein, L.M., Sameoto, D., Hogan, J.D., Asad, A., Dolez, P.I., *Smart Textiles for Visible and IR Camouflage Application: State-of-the-Art and Microfabrication Path Forward*, In: Micromachines, 2021, 12, 7, 773, https://doi.org/10.3390/mi12070773

[5] Rubežiene, V., Minkuviene, G., Baltušnikaite, J., Padleckiene, I., *Development of visible and near infrared camouflage textile materials*, In: Elsevier B.V, 2009, 15, 2, 173–177

[6] Alvi, M.A.H., Maqsood, H., Iftikhar, F., Akhtar, S., Khan, M.Q., Nawab, Y., Kim, I.S., *Fabrication of Multifunctional Tents Using Canvas Fabric*, In: ACS Omega, 2024, 9, 16, 17706–17725, https://doi.org/10.1021/acsomega.3c09249

[7] Md. Anowar, H., *Advancement in UV-Visible-IR camouflage textiles to conceal defence surveillance against multidimensional combat backgrounds*, In: Journal of Materials Science: Materials in Engineering, 2024, 19, 45, https://doi.org/10.1186/s40712-024-00182-8

[8] Gupta, K.K., Nishkam, A., Kasturiya, N., *Camouflage in the Non-Visible Region*, In: Journal of Industrial Textiles, 2001, 31, 1, 27–42, https://doi.org/10.1106/LMQ5-X8LK-27RJ-URPL

[9] Montilla, M., Philips, W., Orjuela-Vargas, S.A., *State of the art of 3D scanning systems and inspection of textile surfaces*, In: Proceedings of SPIE – The International Society for Optical Engineering, 2014, https://doi.org/10.1117/12.2042552

[10] Olaru, S., Popescu, G., Anastasiu, A., Mihaila, G., Salistean, A., *Innovative concept for personalised pattern design of safety equipment,* In: Industria Textila, 2020, 71, 1, 50–54, https://doi.org/10.35530/IT.071.01.1620

[11] Bocancea, V., Marin, I.E., Loghin, C.M., *Multimodal perception of digital protective materials*, In: Industria Textila, 2024, 75, 3, 267–274, http://doi.org/10.35530/IT.075.03.202378

[12] Toma, D., Popescu, G., Popescu, A., Olaru, S., Salistean, A., Badea, I., *Protective clothing system for interventions in emergency situations*, In: Industria Textila, 2023, 74, 1, 121–129, http://doi.org/10.35530/IT.074.01.1839

Authors:

EMILIA VISILEANU, ELENA PERDUM, LAURENTIU DINCA, ADRIAN SALISTEAN, MARIAN CATALIN GROSU

National Research & Development Institute for Textiles and Leather,
16 Lucretiu Patrascanu, 030508, Bucharest, Romania
e-mail: e.visileanu@incdtp.ro, elena.perdum@incdtp.ro, laurentiu.dinca@incdtp.ro,
adrian.salistean@incdtp.ro, catalin.grosu@incdtp.ro

Corresponding author:

EMILIA VISILEANU
e-mail: e.visileanu@incdtp.ro